CHEMISTRY
A EUROPEAN JOURNAL

DOI: 10.1002/chem.200700532

Evidence for Spontaneous Release of Acrylates from a Transition-Metal Complex Upon Coupling Ethene or Propene with a Carboxylic Moiety or CO_2

Michele Aresta,[a] Carlo Pastore,[a] Potenzo Giannoccaro,[a] Gábor Kovács,[b] Angela Dibenedetto,*[a] and Imre Pápai*[c]

Abstract: The development of a new synthetic approach to acrylates based on the formation of alkyl esters of acrylic acids has been studied. A preformed Pd–COOMe moiety is used as a model system to investigate the insertion of an olefin into the Pd–C bond. The fast elimination of acrylate is observed. Density functional calculations support the experimental findings and allow the characterization of transition states along the reaction pathway. The first example of olefin/CO_2 coupling with facile release of ethyl acrylate is also presented.

Keywords: acrylates · density functional calculations · homogeneous catalysis · olefin insertions · polymerization

Introduction

The synthesis of acrylic or methacrylic acid by the direct coupling of olefins (ethene or propene, respectively) and CO_2 has attracted the attention of chemists since the early 1980s.[1–3] Of the metal systems investigated in these pioneering studies, Mo(W)[1] and Ni complexes[2] were shown to promote C–C coupling processes between CO_2 and C_2H_4. The Mo and W complexes[1] were found to have a similar chemistry and afforded dimeric (Mo) or monomeric (W) hydridoacrylate complexes upon coupling ethene and CO_2 (Scheme 1) that were not able to eliminate acrylic acid.

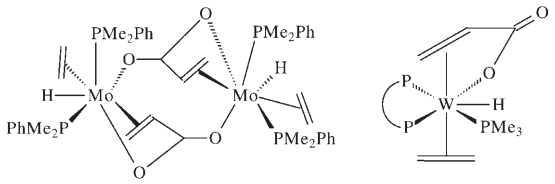

Scheme 1. Mode of bonding of the acrylate moieties formed upon reaction of CO_2 with ethene in the presence of Mo and W.

These complexes afforded propionic acid derivatives upon treatment with dihydrogen or *n*BuLi (Scheme 2). In all cases the original complex was changed into a species that was not able to promote the coupling of ethene and CO_2 for

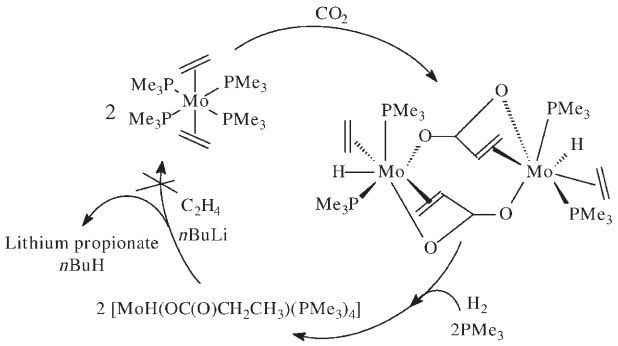

Scheme 2. Displacement of the acrylate moiety by hydrogenation to form propionic acid derivatives.

[a] Prof. M. Aresta, Dr. C. Pastore, Prof. P. Giannoccaro, Prof. A. Dibenedetto
Department of Chemistry – CIRCC and University of Bari
Via Celso Ulpiani, 27, 70126 Bari (Italy)
Fax: (+39) 080-544-3606
E-mail: a.dibenedetto@chimica.uniba.it

[b] Dr. G. Kovács
Research Group of Homogeneous Catalysis
Hungarian Academy of Sciences, University of Debrecen
P.O. Box 7, 4010 Debrecen (Hungary)

[c] Dr. I. Pápai
Chemical Research Center of HAS, Institute of Structural Chemistry
1525 Budapest, P.O.B. 17 (Hungary)
Fax: (+36) 1-325-7554
E-mail: papai@chemres.hu

Supporting Information for this article is available on the WWW under http://www.chemeurj.org/ or from the author.

any significant number of catalytic cycles. Nickel complexes, on the other hand, afforded metallacyclic carboxylates, none of which were able to undergo a β-H shift to generate the acrylate moiety or to eliminate lactones (Scheme 3). These metallacycles afforded propionic acid and $[L_nNiCl_2]$-type

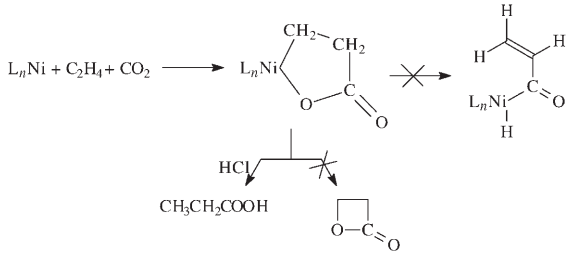

Scheme 3. Reaction of CO_2 with ethene in the presence of Ni.

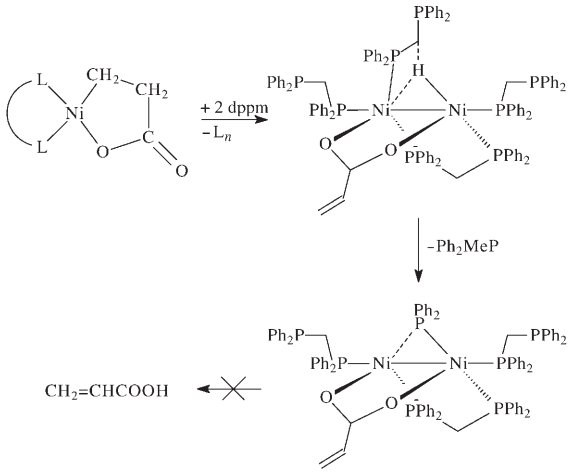

Scheme 4. Reaction of a nickel metallacycle upon treatment with dppm.

complexes upon treatment with HCl.

We have recently examined[4] the mechanism of metal-assisted CO_2/C_2H_4 coupling reactions by means of density functional calculations and have been able to rationalize some of the above findings. We have also shown that the activation barrier of the rate-determining C–C coupling step and the stability of the related intermediates are rather sensitive to the nature of the chelating ancillary ligand.

Nickel metallacycles have very recently been converted into hydridoacrylates in reactions with bis(diphenylphosphino)methane (dppm). These hydridoacrylates then evolved to give dimeric phosphido Ni complexes bearing a bridging acrylate,[5] although no evidence for the release of acrylic acid was obtained in that study either (Scheme 4).

Although the formation of acrylic acid from ethene and CO_2 is thermodynamically allowed under standard conditions, the high bond-dissociation energies of the M–H and M–O moieties in the hydridoacrylate intermediates present substantial kinetic barriers to the elimination of acrylic acid. We have now developed a new synthetic approach that circumvents these kinetic barriers and leads to the formation and elimination of alkyl esters of acrylic acids.

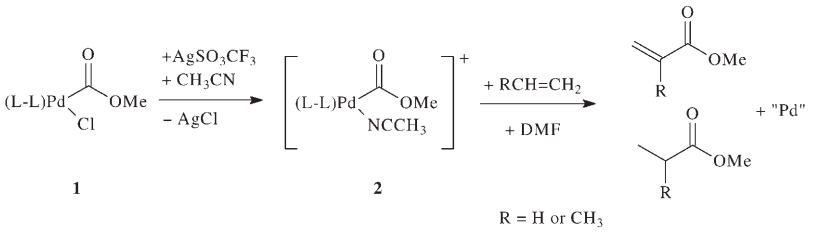

Scheme 5. Pd-mediated coupling of an olefin with the methoxycarbonyl moiety and elimination of acrylates. The saturated derivative is formed in only small amounts.

Results and Discussion

We have used a preformed "Pd–COOMe" moiety as a model system to investigate the insertion of olefins (ethene and propene) into the Pd–C bond and subsequent acrylate elimination (Scheme 5).

Although metalloesters such as **1** or **2** have been known for a long time as they are formed during the methoxycarbonylation of olefins,[6] and the elimination of unsaturated compounds has also been observed in the co-polymerization of CO and olefins,[7] the formation of acrylates has never been investigated in a specific study. We decided to use the complexes [(L–L)PdCl(COOMe)] (L–L = dipyridyl (dipy; **1a**); 2-(2-(diphenylphosphino)ethyl)pyridine (P–N; **1b**); 1,2-bis(diphenylphosphino)ethane (dppe; **1c**)) as parent compounds as we have investigated these complexes extensively for other purposes.[8] These complexes were treated with $Ag(OSO_2CF_3)$ (AgOTf) in CH_2Cl_2/CH_3CN to give the respective cationic complexes $[(L–L)PdCOOMe(CH_3CN)][OTf]$ (**2a–c**).[9]

The IR data for complexes **1a–c** and **2a–c** are listed in Table 1, while key ^1H and ^{31}P NMR spectroscopic data for some of these complexes are given in Tables 2 and 3, respectively.

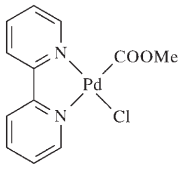

1a

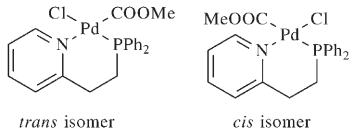

trans isomer *cis* isomer

1b

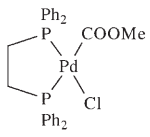

1c

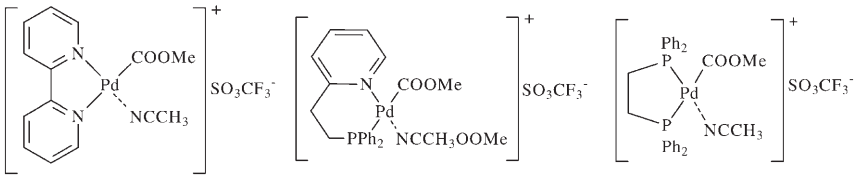

2a 2b 2c

Table 1. IR spectroscopic data for neutral (**1a–c**) and cationic (**2a–c**) complexes [cm^{-1}].

	1a	2a	1b	2b	1c	2c
C=O	1633	1666	1660	1670	1654	1660
C(O)OC	1055	1031	1074	1101	1060	1024
triflate anion	–	1278	–	1265	–	1261
CH_3CN	–	2318	–	2252	–	2293

Table 2. The most significant ^{1}H NMR resonances [ppm] for neutral and cationic complexes.

	1b	2b	1c	2c
m, -CH_2-	2.41–2.49	2.72–2.98	2.71–2.92	2.80–2.91
m (CH_2)	3.46–3.48	3.34–3.44		
s (OCH_3)	3.16	3.16	3.48	3.20
m (aromatic)	7.23–7.85	7.23–7.86	7.53–8.03	7.30–7.77

Table 3. ^{31}P NMR spectroscopic data [ppm] for neutral (**1**) and cationic (**2**) complexes.

Ligand	1	2	
PN	23.87 (*cis* to Cl)	27.57 (*trans* to Cl)	23.93
dppe	32.2 (*trans* to Cl)	47.87 (*cis* to Cl)	39.12

As can be seen from the IR data, the triflate anion is not coordinated in cationic complexes **2a–c**; they bear a coordinated CH_3CN molecule instead. This coordinating solvent is essential to stabilize the cationic complexes as decomposition of the complex occurs very easily if chloride elimination is carried out in the absence of CH_3CN. Table 1 also shows that the formation of the cationic species affects the $\nu_{C=O}$ and ν_{C-OMe} vibrational frequencies because of a charge redistribution on the metal as a result of chloride elimination.

Table 2 lists the ^{1}H NMR spectroscopic data for neutral and cationic complexes **1b**,**c** and **2b**,**c**, respectively. The formation of a positive charge on Pd causes a shift of the resonance of both the methylene moiety of the ancillary ligand and the methyl of the methoxycarbonyl moiety. The ^{31}P NMR signal is also sensitive to elimination of the halide. Formation of the cationic complex eliminates any possible *cis*/*trans* isomerism in **1b** and the phosphorus chemical shift is greatly affected by the positive charge on the Pd atom.

Treatment of the cationic complexes **2a–c** with ethene or propene at room temperature led to the immediate formation of methyl acrylate (MA) or methyl methacrylate (MMA), respectively, in amounts that depend on the ancillary ligand. The yield of organic product increases in the order dipy < P-N < dppe (Table 4).

Formation of the organic compounds was easily detected by their characteristic smell, and they were quantitatively determined by GC-MS and characterized by ^{1}H NMR spectroscopy. The solvent also plays a key role in this reaction, with the highest yields being obtained in dmf (Table 4). Ethene undergoes a faster insertion and produces higher yields of acrylic ester than propene, which gives methyl methacrylate as a single insertion product. The formation of minor amounts of the methyl esters of propionic (from ethene) or 2-methylpropionic acid (from propene) was also observed.

We carried out a more detailed investigation to determine the reaction mechanism (Scheme 6) and rationalize the formation of the saturated esters. With complex **2c**, which affords higher yields, at 250 K we were able to identify the Pd complex **3c**, which bears a coordinated olefin, by ^{1}H NMR spectroscopy and to isolate and characterize the cyclic species **4c** (see Scheme 6 and the Experimental Section). Figure 1 shows the ^{1}H NMR spectroscopic data for coordinated ethene in **3b** and **3c**.

Species **5c** (Scheme 6) could not be isolated as it immediately releases the acrylate. Hydride **7c** could also not be identified in the reaction mixture, most likely because it reacts with either the solvent or the cyclic form **4c** to afford the saturated propionic acid derivative (Scheme 6, left part). This latter reaction is not surprising as we have demonstrated that cationic hydrides of Pd can behave as proton or hydride donors.[10]

We located possible reaction intermediates by performing density functional calculations on various levels of molecular models. According to the gas-phase model (see Figure 2), the initial step of the reaction is the coordination of C_2H_4 to the unsaturated species (**a**), which leads to the ethylene complex (**b**). C–C bond formation between ethyl-

Table 4. Yield of acrylates (with respect to the starting cationic complexes).[a]

Solvent	2a 0.1 MPa of		2b 0.1 MPa of		2c 0.1 MPa of		2c P_{ethene} = 3 MPa	
	ethene	propene	ethene	propene	ethene	propene	P_{CO_2} = 3 MPa	
MA	MMA	MA	MMA	MA	MMA	MA	EA	
CH_2Cl_2	trace	trace	< 0.1 %	trace	11 %	1 %	–	–
CH_2Cl_2/CH_3CN	trace	trace	0.1 %	trace	22 %	5 %	–	–
dmf	trace	trace	1–2 %	trace	85 %	12 %	98 %	> 60 %

[a] MA = methyl acrylate; MMA = methyl methacrylate; EA = ethyl acrylate.

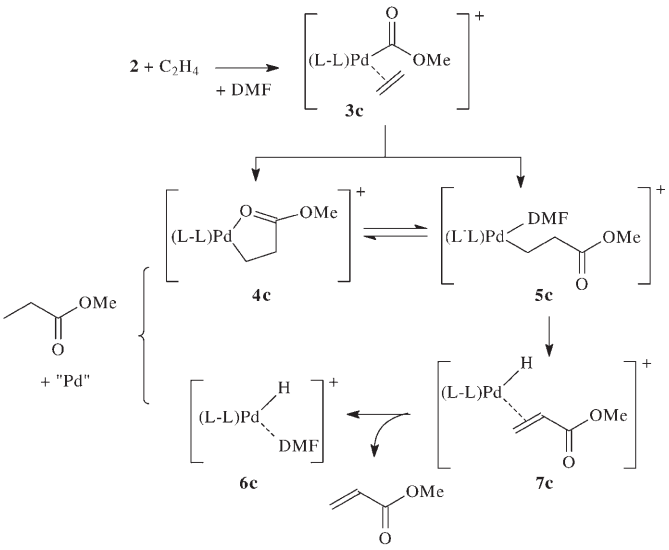

Scheme 6. Proposed mechanism for methyl acrylate formation.

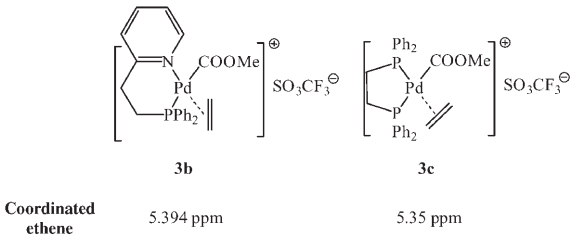

Figure 1. ^{1}H NMR spectroscopic data [ppm] for the coordinated ethene in **3b** and **3c**.

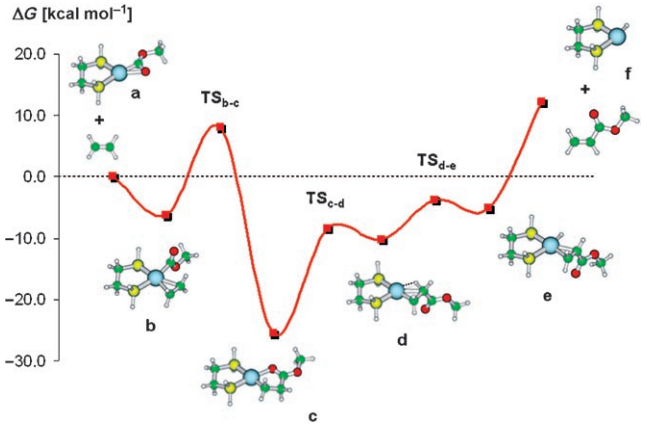

Figure 2. Calculated Gibbs free energy profile for the formation of methyl acrylate (MA) using the gas-phase model.

ene and COOMe takes place via $\mathbf{TS_{b\text{-}c}}$ to give the cyclic metallalactone species (**c**). This step is followed by ring opening via $\mathbf{TS_{c\text{-}d}}$ to give a species with an agostic Pd···(H–C) interaction (**d**), which is followed by a β-hydrogen shift via $\mathbf{TS_{d\text{-}e}}$ to give the hydridoacrylate intermediate (**e**). Finally, dissociation of the acrylate moiety from **e** leads to the unsaturated hydride species **f**.

The gas-phase model predicts a highly endergonic process for the overall reaction with $\Delta G = +12.2$ kcal mol^{-1}. The metallacyclic species is calculated to be substantially more stable than the observed products, which leads us to conclude that gas-phase calculations do not represent a reliable model for the acrylate formation.

The solvated model, on the other hand, which explicitly considers the solvent molecule dmf and includes the effect of bulk solvent via a dielectric continuum model, resulted in energetics that are consistent with the experimental findings (Figure 3). dmf forms relatively strong bonds with the metal

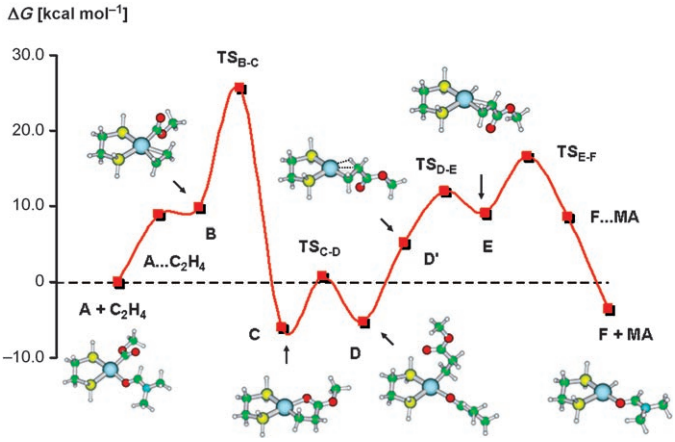

Figure 3. Calculated free energy profile for the formation of methyl acrylate (MA) using the solvated model. For the sake of clarity, the dmf molecule has been omitted for structures **B**, **C**, **D′** and **E** as it interacts only weakly with the metal centre. The full structures are given in the Supporting Information. Letters A–F are correlated to a–f in Figure 3 but not to a–c in the labeling of the complexes.

centre of unsaturated cationic species, including the parent $[(L{-}L)Pd(COOMe)]^+$ and $[(L{-}L)PdH]^+$ hydride complexes, thereby giving rise to square-planar complexes **A** and **F**, respectively (see Figure 4). The explored reaction pathway involves the formation of ethene complex **B** via the weakly bonded species **A**···C_2H_4, which is followed by the rate determining C–C coupling process (via $\mathbf{TS_{B\text{-}C}}$) to yield the metallacycle **C**. The ring opening in **C** (via $\mathbf{TS_{C\text{-}D}}$) occurs easily because the open form of this species (**D**) is stabilized by coordination of dmf to Pd. The β-H shift takes place via an agostic intermediate **D′** and transition state $\mathbf{TS_{D\text{-}E}}$, which allows the formation of a hydride complex that bears the acrylate ester coordinated through its double bond (**E**). Dissociation of the acrylate is facilitated by the solvent that coordinates to Pd in hydride species **F**. The overall coupling reaction is predicted to be clearly exergonic using the solvated model ($\Delta G = -3.5$ kcal mol^{-1}) due to the enhanced stability of the coordinatively saturated hydride **F** with respect to **A**. As there is no direct solvent stabilization in structure **C**, the free-energy of the cyclic species becomes comparable to that of the products. Our calculations thus underline the importance of the solvent molecules in the reaction, which is in perfect agreement with the experimental findings.

To verify whether the Pd hydride formed in the reaction would be able to initiate a catalytic cycle for possible CO_2/olefin coupling processes, we heated complexes **2a–c** at 300 K under variable pressures of olefin and CO_2. We discovered that complex **2c** gives rise to two clearly distinguished classes of acrylates with ethene under these conditions, namely the methyl and ethyl ester of acrylic acid. While formation of the methyl ester can be rationalized in terms of Scheme 5 and is supported by density functional calculations (Figure 4), the ethyl ester must have a different origin and necessarily requires the reaction of ethene and CO_2. Furthermore, the overall molar ratio of acrylic esters/Pd increases well above 1 (>1.6). The yield of methyl ester is almost quantitative with respect to the amount of Pd complex used, whereas the yield of ethyl ester increases with the pressure of ethene (Table 4) and the yield of propionic derivatives decreases significantly, approaching zero. The yield of ethyl ester is zero at 0.1 MPa of the olefin in the absence of CO_2 and higher than 60% with respect to Pd under 3 MPa of ethene and 3 MPa of CO_2.

A logical explanation for the formation of ethyl acrylate would be the reaction sequence shown in Scheme 7, which

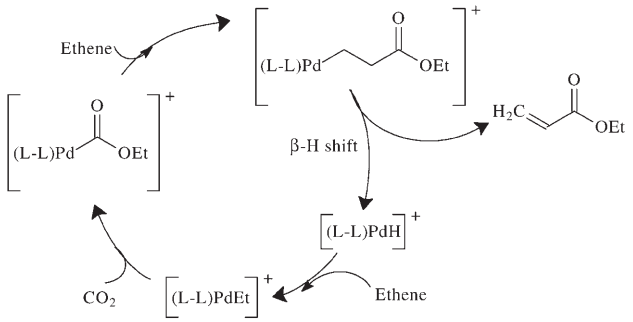

Scheme 7. A putative mechanism for the synthesis of acrylates from CO_2 and ethene catalysed by "LnPd–H" species (L–L = dppe).

includes ethene insertion into $[(L{-}L)PdH]^+$ and subsequent insertion processes with CO_2 and C_2H_4. The insertion of CO_2 into a Pd–Me bond has been reported by Wendt et al.[11] to yield a Pd–$OCOCH_3$ (acetate) fragment instead of a Pd–COOR (alkoxycarbonyl) fragment. Our density functional calculations indicate that although the $[(L{-}L)PdEt]^+$ intermediate can form easily, the so-called "inverse" CO_2 insertion into the Pd–Et bond takes place via a high energy barrier (58 kcal mol^{-1}, see Figure 4),[12] which practically excludes this reaction pathway. This is further confirmed by the fact that preformed alkylpalladium complexes do not react with CO_2 and ethene to afford acrylates under the conditions reported in the Experimental Section. A more complex and unusual mechanism involving new, non-trivial intermediates should therefore be proposed for the formation of ethyl acrylate esters from ethene and CO_2. Theoretical studies along these lines are in progress in our group.

As we were still lacking computational support for a possible mechanism for the formation of the ethyl esters we carried out experiments using ethene and $^{13}CO_2$ in the presence of **2c**. The products isolated were $CH_2{=}CHCOOCH_3$ (almost quantitative yield), which is formed directly from **2c** following the reaction path shown in Scheme 5, and $CH_2{=}CH^{13}COOEt$, which can only be formed by coupling $^{13}CO_2$ with ethene, whatever the mechanism. This is the first clear demonstration of the coupling of ethene and CO_2 to afford ethyl acrylate rather than acrylic acid. The yield of more than 60% is not low, as is the case under mild conditions, and the ethyl ester bearing $^{13}CO_2$ can only be formed from the original Pd complex **2c**, ethene and $^{13}CO_2$. However, to further prove this assumption we treated the cationic complex **2c** with $^{13}CO_2$ and did not observe any incorporation of $^{13}CO_2$ into the methyl ester.

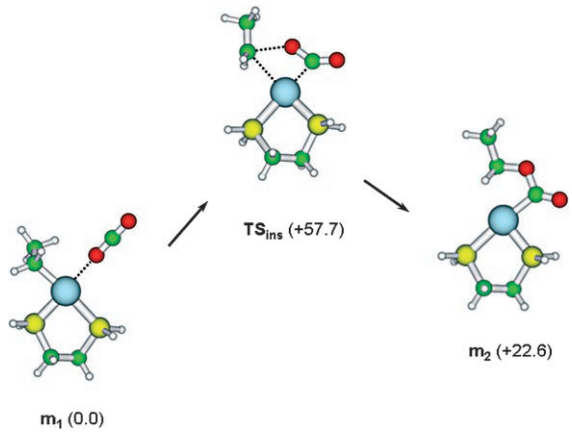

Figure 4. Located structures and their relative energies [kcal mol^{-1}] for an assumed CO_2 insertion process.

As the amount of esters formed upon coupling ethene and CO_2 is not low, further investigations (covering both experimental and theoretical aspects) are in progress to elucidate the mechanistic details and to improve the conversion efficiency of ethene and CO_2 into acrylate.

Conclusion

In summary, our results demonstrate that esterification of the carboxylic moiety prevents the formation of M–H and M–O bonds and makes release of an acrylate or methacrylate moiety from a metal centre possible. Such findings may be of great interest for developing a new route to acrylates from olefins and CO_2. Ethyl acrylate has been shown to be formed from ethene and CO_2 for the first time.

Experimental Section

All solvents were RP-grade Aldrich reagents and were distilled[13] and stored under dinitrogen (99.98% quality). High-pressure reactions were carried out in a custom built stainless-steel 4xparallel reactor. IR spectra were recorded with an FTIR Shimadzu IR Prestige-21 apparatus. GC-MS analyses were carried out with a Shimadzu 17 A gas chromatograph (capillary column: 30 m; MDN-5S; diameter: 0.25 mm, 0.25 μm film) cou-

pled to a Shimadzu QP5050 A mass spectrometer. Quantitative determinations on the reaction solutions were performed with a Hewlett–Packard 6850 GC-FID (capillary column: 30 m; MDN-5S; diameter: 0.25 mm, 0.25 μm film).

Synthesis of neutral complexes: Neutral compounds **1a–c** (Figure 1) were prepared as reported in the literature.[14] The procedure for **1a** was optimized as follows: An excess of triethylamine (1.2 mL, 8.75 mmol) was added to a suspension of [(dppe)$PdCl_2$] (656 mg, 1.2 mmol) in dry methanol (15 mL) and the reaction mixture was stirred for 10 h at 45 °C under an atmosphere of CO. During this time the color of the reaction mixture changed from white to brown. The solid formed was filtered off, washed with methanol (2×5 mL) and dried under vacuum. Yield: 70% (480 mg). Elemental analysis calcd (%) for $C_{28}H_{27}ClO_2P_2Pd$: C 56.12, H 4.54, Cl 5.91, P 10.35, Pd 17.77; found: C 56.09, H 4.61, Cl 5.88, P 10.29, Pd 17.87.

Complexes **1b**,**c** gave correct elemental analyses and their IR and NMR spectra were in agreement with the literature data. The IR and NMR spectroscopic data of compounds **1a–c** are reported in Tables 1, 2 and 3.

Synthesis of cationic complexes: The following general procedure was used to synthesise the cationic complexes **2a–c**. The neutral complex (**1a–c**; 0.4 mmol) was dissolved in a mixture of dichloromethane (15 mL) and CH_3CN (8 mL) then a stoichiometric amount of a standardized solution (0.09 M) of AgOTf in CH_3CN was slowly added. After stirring for 15 min the AgCl formed was separated by filtration and the filtrate was concentrated under vacuum to half its volume. The solid product formed was isolated by filtration, washed with CH_2Cl_2 (2×2 mL) and dried in vacuo.

2a: Elemental analysis calcd (%) for $C_{13}H_{14}F_3N_2O_5PdS{\cdot}C_2H_3N$: Pd 20.68; found: Pd 20.62.

2b: Elemental analysis calcd (%) for $C_{22}H_{21}F_3NO_5PPdS{\cdot}C_2H_3N$: P 4.79, Pd 16.45; found: P 4.68, Pd 15.98.

2c: Elemental analysis calcd (%) for $C_{29}H_{27}F_3O_5P_2PdS{\cdot}C_2H_3N$: P 8.37, Pd 14.38; found: P 8.42, Pd 14.83.

C, H, N analyses were not reliable as the complexes are strongly hygroscopic and were weighed in air. CH_3CN was instead determined by displacement from the parent complex with hydrogen chloride (HCl) under nitrogen and analyzed by quantitative GC analysis.

2a: CH_3CN (%) calcd 8.85; found: 8.38.

2b: CH_3CN (%) calcd 6.87; found: 6.44.

2c: CH_3CN (%) calcd 5.64; found 5.28.

IR and NMR spectroscopic data for the cationic complexes (**2a–c**) are reported in Tables 1, 2 and 3.

Reaction of the cationic complexes with olefins: The general procedure for the reaction of the cationic complexes with ethene or propene is as follows. The cationic complex **2a–c** was prepared in situ as described above. After separation of the AgCl by filtration, the filtrate was stirred under 0.1 MPa of ethene (or propene) at room temperature. The solution was then analyzed by GC-MS and the acrylate (or methyl methacrylate) formed was quantitatively determined. When the reaction of the cationic complex with ethene was carried out in an NMR tube at 250 K formation of the cationic ethene complexes was supported by the appearance of signals for coordinated ethene at $\delta = 5.39$ (**3b**) and 5.35 ppm (**3c**). In the latter case, the cyclic complex **4c** was isolated as a yellowish solid in low yield. ^{1}H NMR ([D_7]dmf, 400 MHz): $\delta = 0.75$–1.28 (m, 4H; -PdCH_2CH_2CO-), 2.64 (s; dmf), 2.81 (s; dmf), 2.91–3.15 (br. s, 4H; Ph_2PCH_2CH_2PPh_2), 3.41 (s, 3H; -OCH_3), 7.33–7.62 (m, 20H; *o*-, *m*-, *p*-Ph dppe), 7.81 ppm (s; dmf).

When the solution containing the cationic complex was transferred into a stainless-steel autoclave that was charged with ethene up to 3 MPa and CO_2 up to 3 MPa, both methyl and ethyl acrylate were formed. The yields of acrylates, as determined by GC-MS analysis, are reported in Table 4. Methyl acrylate, methyl methacrylate and ethyl acrylate were identified by GC-MS by comparison with pure samples.

Methyl acrylate: *m*/*z*: 85 [M^+], 58, 55, 42, 31.

Methyl methacrylate: *m*/*z*: 100 [M^+], 99, 85, 69, 55, 41, 31, 29.

Ethyl acrylate: *m*/*z*: 99, 85, 73, 55, 45, 29.

The formation of ethyl acrylate from ethene and $^{13}CO_2$ was evident from the isotopic labelling of some peaks in the mass spectrum of the product. As $^{13}CO_2$ contains approximately 3% of $^{13}C^{16}O^{18}O$, the moieties containing oxygen also show peaks that are two mass units higher (given in parentheses).

^{13}C-Ethyl acrylate: *m*/*z* 100 (103) [M^+], 100 (102) [M^+−H], 86 (88) [M^+ −CH_3], 56 (58) [CH_2=CHCO], 45 (47) [CH_3CH_2O], 29, 27.

Computational details: Density functional theory was applied at the B3LYP/SDDP level to characterize the electronic structure of the species assumed to be involved in the reactions. B3LYP refers to the approximated exchange-correlation functional[15–17] and SDDP denotes a basis set including the Stuttgart–Dresden relativistic small core ECP basis set for Pd and the Dunning/Huzinaga DZ + polarization all-electron basis set for the lighter atoms.[18–21]

The chelating dppe ligand in the cationic palladium complexes was replaced by $H_2P(CH_2)_2PH_2$ (dpe) to keep the quantum chemical calculations within reasonable limits. Test calculations carried out for some of the full structures indicated that the error introduced by this structural simplification concerning the relative energies of the reaction intermediates is about 2 kcal mol^{-1}. The structures of all species investigated were fully optimized and the transition states of assumed elementary steps were located. Vibrational frequencies were calculated for each located stationary point to characterize their nature and to estimate the zero-point energy and thermal contributions to the gas-phase free enthalpy of the reaction components. Thermal corrections were calculated assuming standard conditions ($T = 298$ K and $p = 0.1$ MPa).

The solvent effects were included by explicit treatment of a single solvent molecule (dmf), which was allowed to interact with the metal complexes. These structures were also fully optimized and the free enthalpies of located stationary points (G_g) were obtained as described above. Furthermore, the effect of bulk solvent was estimated in terms of self-consistent reaction field (SCRF) calculations using the PCM-UA0 solvation model.[22,23] The dielectric constant in the SCRF calculations was set to $\varepsilon = 39.0$ to simulate dmf as a solvent. The reported energetics for the solvated model were computed as $G = G_g + G_s$, where G_s refers to the free energies of solvation obtained from the PCM-UA0 calculations.

All calculations were carried out with the Gaussian 03 package.[24]

Acknowledgments

The Italian authors thank Dr. V. Schiralli for experimental assistance, the University of Bari and MUR (contract 2006031888) for financial support. The Hungarian authors acknowledge a Hungarian Research Grant (K60549).

[1] a) R. Alvarez, E. Carmona, D. J. Cole-Hamilton, A. Galindo, E. Gutierrez-Puebla, A. Monge, M. L. Poveda, C. Ruiz, *J. Am. Chem. Soc.* **1985**, *107*, 5529–5531; b) R. Alvarez, E. Carmona, A. Galindo, E. Gutierrez, J. M. Marin, A. Monge, M. L. Poveda, C. Ruiz, J. M. Savariault, *Organometallics* **1989**, *8*, 2430–2439; c) A. Galindo, A. Pastor, P. J. Perez, E. Carmona, *Organometallics* **1993**, *12*, 4443–4451.

[2] a) H. Hoberg, D. Schäfer, *J. Organomet. Chem.* **1983**, *251*, C15–C17; b) H. Hoberg, D. Schäfer, G. Burkhart, C. Krüger, M. J. Romaõ, *J. Organomet. Chem.* **1984**, *266*, 203–224; c) H. Hoberg, K. Jenni, C. Angermund, C. Kruger, *Angew. Chem.* **1987**, *99*, 141–142; *Angew. Chem. Int. Ed. Engl.* **1987**, *26*, 153–155; d) H. Hoberg, Y. Peres, C. Krüger, Y. Tsay, *Angew. Chem.* **1987**, *99*, 799–800; *Angew. Chem. Int. Ed. Engl.* **1987**, *26*, 771–772.

[3] *Industrial Organic Chemistry* (Eds.: K. Weissermel, H.-J. Harpe), Wiley-VCH, Weinheim, **2003**.

[4] a) I. Pápai, G. Schubert, *J. Am. Chem. Soc.* **2003**, *125*, 14847–14858; b) I. Pápai, G. Schubert, I. Mayer, G. Besenyei, M. Aresta, *Organometallics* **2004**, *23*, 5252–5259.

[5] R. Fischer, J. Langer, A. Malassa, D. Walther, H. Görls, G. Vaughan, *Chem. Commun.* **2006**, 2510–2512.
[6] a) J. Liu, B. T. Heaton, J. A. Iggo, R. Whyman, J. F. Bickley, A. Steiner, *Chem. Eur. J.* **2006**, *12*, 4417–4430; b) G. Cavinato, L. Toniolo, A. Vavasori, *J. Mol. Catal. A: Chem.* **2004**, *219*, 233–240, and references therein; c) S. Otsuka, A. Nakamura, T. Yoshida, M. Naruto, K. Ataka, *J. Am. Chem. Soc.* **1973**, *95*, 3180–3188; P. W. N. M. van Leeuwen, M. A. Zuideveld, B. H. G. Swennenhuis, Z. Freixa, P. C. J. Kamer, K. Goubitz, J. Fraanje, M. Lutz, A. L. Spek, *J. Am. Chem. Soc.* **2003**, *125*, 5523–5539, and references therein.
[7] M. Sperrle, G. Consiglio, *J. Mol. Catal. A: Chem.* **1999**, *143*, 263–277.
[8] a) P. Giannoccaro, D. Cornacchia, S. Doronzo, E. Mesto, E. Quaranta, M. Aresta, *Organometallics* **2006**, *25*, 2872–2879; b) M. Aresta, P. Giannoccaro, I. Tommasi, A. Dibenedetto, A. Manotti, F. Ugozzoli, *Organometallics* **2000**, *19*, 3879–3889.
[9] M. Aresta, A. Dibenedetto, P. Giannoccaro, V. Schiralli, I. Pápai, G. Kovács, *CO.GI.CO Meeting*, Paper O4, Parma, Italy, 9–12 July, **2006**.
[10] M. Aresta, A. Dibenedetto, I. Pápai, G. Schubert, A. Macchioni, D. Zuccaccia, *Chem. Eur. J.* **2004**, *10*, 3708–3716.
[11] R. Johansson, M. Jarenmark, O. F. Wendt, *Organometallics* **2005**, *24*, 4500–4502.
[12] We examined the effect of the various approximations applied in our model (simplification of dppe ligand, solvent effect, etc.) and did not find a notable reduction for the insertion barrier.
[13] D. D. Perrin, W. L. F. Armarego, D. R. Perrin, *Purification of Laboratory Chemicals*, Pergamon Press, Oxford, England, **1986**.
[14] a) P. Giannoccaro, N. Ravasio, M. Aresta, *J. Organomet. Chem.* **1993**, *451*, 243–248; b) R. Bertani, G. Cavinato, L. Toniolo, G. Vasapollo, *J. Mol. Catal.* **1993**, *84*, 165–176.
[15] A. D. Becke, *J. Chem. Phys.* **1993**, *98*, 5648–5652.
[16] C. Lee, W. Yang, R. G. Parr, *Phys. Rev. B* **1988**, *37*, 785–789.
[17] P. J. Stephens, F. J. Devlin, C. F. Chabalowski, M. J. Frisch, *J. Phys. Chem.* **1994**, *98*, 11623–11627.
[18] M. Dolg, H. Stoll, H. Preuss, R. M. Pitzer, *J. Phys. Chem.* **1993**, *97*, 5852–5859.
[19] T. H. Dunning, Jr., *J. Chem. Phys.* **1970**, *52*, 2823–2833.
[20] T. H. Dunning, Jr., P. J. Hay, *Methods of Electronic Structure Theory, Vol. 3* (Ed.: H. F. Schaefer, III), Plenum Press, New York, USA, **1977**.
[21] H. F. Schaefer, III, *J. Chem. Phys.* **1985**, *83*, 5721–5726.
[22] S. Miertus, E. Scrocco, J. Tomasi, *J. Chem. Phys.* **1981**, *55*, 117–129.
[23] V. Barone, M. Cossi, J. Tomasi, *J. Chem. Phys.* **1997**, *107*, 3210–3221.
[24] M. J. Frisch, G. W. Trucks, H. B. Schlegel, G. E. Scuseria, M. A. Robb, J. R. Cheeseman, J. A. Montgomery, Jr., T. Vreven, K. N. Kudin, J. C. Burant, J. M. Millam, S. S. Lyengar, J. Tomasi, V. Barone, B. Mennucci, M. Cossi, G. Scalmani, N. Rega, G. A. Petersson, H. Nakatsuji, M. Hada, M. Ehara, K. Toyota, R. Fukuda, J. Hasegawa, M. Ishida, T. Nakajima, Y. Honda, O. Kitao, H. Nakai, M. Klene, X. Li, J. E. Knox, H. P. Hratchian, J. B. Cross, C. Adamo, J. Jaramillo, R. Gomperts, R. E. Stratmann, O. Yazyev, A. J. Austin, R. Camml, C. Pomelli, J. W. Ochterski, P. Y. Ayala, K. Morokuma, G. A. Voth, P. Salvador, J. J. Dannenberg, V. G. Zakrzewski, S. Dapprich, A. D. Daniels, M. C. Strain, O. Farkas, D. K. Malick, A. D. Rabuck, K. Raghavachari, J. B. Foresman, J. V. Ortiz, Q. Cui, A. G. Baboul, S. Clifford, J. Cioslowski, B. B. Stefanov, G. Liu, A. Liashenko, P. Piskorz, I. Komaromi, R. L. Martin, D. J. Fox, T. Keith, M. A. Al-Laham, C. Y. Peng, A. Nanayakkara, M. Challacombe, P. M. W. Gill, B. Johnson, W. Chen, M. W. Wong, C. Gonzalez, J. A. Pople, Gaussian 03, revision C.02, Gaussian, Inc.: Pittsburgh, PA, **2004**.

Received: April 4, 2007
Revised: June 21, 2007
Published online: August 15, 2007

